

CrystEngComm

Accepted Manuscript



This is an *Accepted Manuscript*, which has been through the Royal Society of Chemistry peer review process and has been accepted for publication.

Accepted Manuscripts are published online shortly after acceptance, before technical editing, formatting and proof reading. Using this free service, authors can make their results available to the community, in citable form, before we publish the edited article. We will replace this *Accepted Manuscript* with the edited and formatted *Advance Article* as soon as it is available.

You can find more information about *Accepted Manuscripts* in the [Information for Authors](#).

Please note that technical editing may introduce minor changes to the text and/or graphics, which may alter content. The journal's standard [Terms & Conditions](#) and the [Ethical guidelines](#) still apply. In no event shall the Royal Society of Chemistry be held responsible for any errors or omissions in this *Accepted Manuscript* or any consequences arising from the use of any information it contains.

**Self-assembly process of China rose-like β -Co(OH)₂ and its
Topotactic Conversion Route to Co₃O₄ with optimizable
catalytic performance**

Xiangming Xu¹, Yongjie Zhao^{1*}, Yuzhen Zhao², Heping Zhou², Fida Rehman¹, Jingbo

Li¹ and Haibo Jin^{1*}

¹School of Materials Science and Engineering, Beijing Institute of Technology,

Beijing 100081, China

²State Key Laboratory of New Ceramics and Fine Processing, School of Materials

Science and Engineering, Tsinghua University, Beijing, 100084, China

* Authors to whom correspondence should be addressed. Electronic mail:

zhaoyjpeace@gmail.com and hbjin@bit.edu.cn

ABSTRACT

China rose-like structured β -Co(OH)₂ were fabricated by a facile and surfactant free solvothermal method. Self-assembly process of 3D flower-like structure was preliminarily explored via time-dependent observation. The chemical transformation achieved by thermal treatment from brucite-like β -Co(OH)₂ to spinel Co₃O₄ was investigated in detail, while the original flower-like framework of precursor was preserved during the whole process. With the increase in the temperature of heat treatment, specific surface area decreased correspondingly. Meanwhile, cracks propagation and following cavitation progress were realized on petal-like flakelets. Topotactic nucleation and crystallization with [111] direction of spinel-structured Co₃O₄ inheriting the [0001] direction of hexagonal structured β -Co(OH)₂ were analyzed in detail. The catalytic performance of obtained Co₃O₄ materials on the thermal decomposition of ammonium perchlorate (AP) was analyzed. It was fortunately found that samples annealed at 280 °C could lower the thermal decomposition temperature of AP from 450 °C to 245 °C, when obtained Co₃O₄ occupied 4% w/w of the mixture. This excellent performance renders great practical significance in the development of solid rocket fuel.

Key words: China rose-like; β -Co(OH)₂; spinel Co₃O₄; thermal treatment; specific surface area; catalytic properties; ammonium perchlorate.

1. Introduction

The cobalt oxide, one of magnetic transition metal oxides, presents broad engineering application in several fields, such as secondary batteries,^{1, 2} super capacitors,³ gas sensor,⁴ catalyst^{5, 6} and magnetic device.⁷ This is not only because of its intriguing magnetic, optical, electronic, and electrochemical properties, but also its normal spinel structure denoted as AB_2O_4 as well as the possibility of being prepared into various morphologies in micro-nano scale.⁶ Micro/nano Co_3O_4 materials with various morphologies have been synthesized. Chen et al prepared Co_3O_4 nanotubes, nanodiscs, and nanoflowers as well as the comparison and analysis their Lithium-Storage properties.⁸ Ghosh et al. prepared platelet Co_3O_4 through the calcination of the Platelet $\beta-Co(OH)_2$.³ Other kinds of morphology were also well achieved, such as Co_3O_4 nanobelts,⁹ nanosphere,¹⁰ nanoplate,¹¹ nanowire,¹² nanocube,¹³ and so forth. Moreover, recently micro/nano materials with different flower shapes were synthesized and investigated due to their great specific surface area and mesoporous microstructure. Li et al. fabricated Co_3O_4 nano-flower clusters by low-temperature hydrothermal method and catalytic oxidation of gaseous toluene was also studied with the obtained product.⁶ Jadhav et al. achieved flower-like Co_3O_4 assembled by nano-rod with the approach of chemical co-precipitation followed by a heat treatment and its high performance as an anode in lithium-ion batteries was researched.¹

Ammonium perchlorate (AP) was widely used as a common oxidant in solid composite propellants because of its unique thermal decomposition characteristics. However, the complete decomposition of AP is required at relatively high temperature

(>420 °C) and its high temperature decomposition is complex and dangerous.¹⁴ Thus, the research of utilizing transition metal oxides as catalyst in the thermal decomposition reaction of AP is of positive significance in the development of energy-efficient solid propellant formulations. Hu et al. reported that the Mn₃O₄-GR hybrids decreased by 141.9 °C (422-278.1 °C).¹⁴ Micron-sized MnO₂ lowers the peak temperature from 426.3 °C to 341.2 °C.¹⁵ The Fe₂O₃/grapheme nano-composite can decrease the decompose temperature to 367 °C,¹⁶ nano-sized MgO flakes can reduce the peak temperature to 354.7 °C.¹⁸ Co₃O₄ micro-spheres transformed from CoCO₃ particles were reported decreasing reaction temperature to 320 °C.¹⁹

In current work, flower-like Co₃O₄ were achieved via annealing China rose-like β-Co(OH)₂, which was firstly synthesized by template-free, surfactant-free solvothermal method. Taking flower-like Co₃O₄ as catalyst, temperature decomposition of AP was lowered to below 250 °C, which is better than any reported catalyst on this item. Structures and morphologies of this kind sample which showed very promising performance as high-energy fuel catalysts were deeply analyzed.

2. Experiment

2.1 Materials and Synthesis

All chemicals, 1, 2-propylene (CH₂OHCHOHCH₃), sodium hydroxide (NaOH) and cobalt acetate tetrahydrate (C₄H₆CoO₄·4H₂O), ammonium perchlorate (AP) were commercial products with analytical grade without further purification.

Synthesis of the Precursor: In a typical synthesis of the precursor cobalt hydroxide, i.e., β-Co(OH)₂, 3 mmol of C₄H₆CoO₄·4H₂O was dissolved into 20 ml of 1,

2-propanediol to form a homogeneous solution. Sodium hydroxide aqueous solution was made up with the pH value 10. And then, these two kinds of solutions were mixed together with 30 minutes of magnetic stirring. The reaction mixture was consequently transformed into a 50 ml Teflon-lined stainless steel autoclave. The sealed autoclave was heated to 220 °C and held for 24 h. After being cooled down to ambient temperature, the β -cobalt hydroxide precursor was filtered and thoroughly washed with distilled water and ethanol several times, and then dried in the oven before further characterization.

Preparation of flower-like Co_3O_4 products: the as-synthesized β -cobalt hydroxide precursor was converted into pure spinel Co_3O_4 phase by the calcination. The typical heating process was carried out in a crucible without using any inert gases for protection, and the temperature was increased up to designed temperature with the speed of 1 °C/min, and then maintained for 2 h.

2.2 Characterization

The structure and phase of the samples were examined by X-ray diffraction (XRD, D8/ADVANCE diffractometer, Cu K_α $\lambda=1.5418$ Å). The microstructure was observed on the field emission scanning electron microscope (SEM, LEO-1530, Oberkochen, Germany, LEO-1530) and transmission electron microscope (TEM, JEM-2100F). The BET surface area was estimated using adsorption data in a relative pressure range from 0.08 to 0.3 according to the desorption data of the N_2 isotherm. The catalytic properties of samples concerning the thermal decomposition of AP were tested through Thermo Gravimetric Analyzer (N33-TG 209 F3), in which the mass

percentage of selected Co_3O_4 sample was 4%.

3. Results and Discussion

The reaction of cobalt acetate and ammonia in a mixture of water and 1, 2-propanediol at 220 °C can yield China rose-like structured $\beta\text{-Co(OH)}_2$. SEM images of $\beta\text{-Co(OH)}_2$ with different magnifications showing morphology and self-assembled structure were provided in Fig. 1(a)-(c) and lower magnification SEM images were supported Fig. S1. Large quantities of the typical China rose-like particles with a size of about 15 μm were clearly revealed by low-magnified SEM images. Samples also contained a certain quantity of small particles and petal-like chips. A closer observation in Fig. 1(b)-(c) exhibited that each flower was of orderly hierarchical structure and composed of thin nano-sheet with the thickness of less than 60 nm. The surface and cross-section of nano-sheet were very smooth. All the diffraction peaks of the flower-like product as revealed in Fig. 1(d) are well indexed as the brucite-like $\beta\text{-Co(OH)}_2$ according to JCPDS Card No. 30-0443. Product showed good crystallinity and preferred along the [001] orientation in XRD pattern. No other impurity phase was detected in XRD patterns. Good uniformity in thickness of nano-sheet was displayed in bright field of TEM image shown in Fig. 1(e). Interestingly, Good single-crystal-like alignment state of the nano-sheet was further verified by HRTEM image (Fig. 1(f)) and the corresponding electron diffraction (SAED) pattern in red-marked area in Fig. 1(e). Two orthogonal crystal planes of $\beta\text{-Co(OH)}_2$, (100) corresponding to the d value of 0.269 nm and (002) corresponding to 0.232 nm, were observed from HRTEM image. The corresponding electron

diffraction pattern interpreted its single crystal pattern with several families of crystal planes $\{100\}$, $\{110\}$ and $\{200\}$.

Since this method is very effective for the synthesis of β -Co(OH)₂ with 3D flower-like structure, the growth process was monitored by time-dependent observation. Fig. 2(a)-(c) showed the SEM images of the samples obtained after reaction for 2, 12 and 24 h, respectively. Fig. 2(a) revealed hexagonal micro-disk formed in initial stage. The β -Co(OH)₂ bulk materials possess a hexagonal structure. It is a layered compound composed of a Co layer sandwiched by two O layers.²⁰ Therefore, Co(OH)₂ prefers to grow into platelets due to their intrinsic lamellar structures,²¹ and XRD pattern for 2h presented in Fig. S2 indicated obvious orientation along [001]. When the reaction time was extended to 12 h (Fig. 2(b)), petaloid micro-platelet gradually formed from Ostwald ripening of micro-disk. Parts of micro-platelet were assembled into flower-like particle. When reaction time was further extended to 24 h, self-assembly process was ongoing and most of β -Co(OH)₂ transformed into China rose-like micro-flower. Corresponding XRD patterns (Fig. S2) indicated all of them with pure hexagonal β -Co(OH)₂ structure, and orientation changed along the direction of [101].

The whole growth process was simply depicted in Fig. 2(d). The first step is the formation and growth of β -Co(OH)₂ microdisk. Then with the high temperature and pressure environment in reaction kettle, β -Co(OH)₂ microdisk underwent the shape evolution. Then, The nano petal that self-assembly processed into β -Co(OH)₂ flowers was finished with the reconstruction of crystal structure. The whole process was with

growing orientation along [101]. However, the exact mechanism for the formation of these complex hierarchical structured β -Co(OH)₂ is still need further investigation.

Co(OH)₂ sample was calcined in the electrical oven in air atmosphere and the selected heat treatment temperature were 280, 360, 400, 440, and 520 °C, respectively. The crystal structural transformation from Co(OH)₂ to Co₃O₄ had been checked by XRD. XRD patterns in Fig. 3 showed that phase-pure Co₃O₄ could be obtained above 280 °C. With the increase of heat treatment temperature, the relative intensity of the diffraction peaks became stronger. Meantime the full width at half maximum (FWHM) of the diffraction peaks became narrower, indicating the increase of the crystallinity. Furthermore, these diffraction peaks of all the annealed samples were perfectly indexed to a standard Co₃O₄ phase (JCPDS No. 42-1467) with a space group of Fd3m (227). The lattice parameters of the corresponding Co₃O₄ cubic spinel structure could be primarily identified with $a=b=c=3.14 \text{ \AA}$.

The typical morphology of Co₃O₄ obtained by calcining the Co(OH)₂ precursor at a series of temperature was observed by low magnification TEM and SEM. It is clear that the flower-like sketch of the products was preserved after calcination, and this was well displayed in large scale SEM images of products at different calcination temperature in Fig. S3(a-f). However, nano-plate which was units assembling into micro-flower showed some interesting transformations. Surfaces of nano-sheet in β -Co(OH)₂ precursor were smooth and compact as shown in Fig. 4(a). Nano-sheet Co₃O₄ samples annealing at 280 °C were rough and accompanied with the appearance of small cracks (Fig. 4(b)). With the increase of heat treatment

temperature from 280 °C to 440 °C, cracks began to expand and became pretty large in size as shown in Fig. 4(c-e). When the temperature of thermal treatment reached up to 520 °C, cracks in the surface of nano-sheet completely transformed into nano-sized pores. Fine texture change mechanism of nano-petals was figured out by analyzing low magnification TEM images in Fig. 4(a-f), just as shown in Fig. 4(g). With the increase of annealing temperature, nano-petals started to crack, followed by the expansion of the crack, and finally the crack changed into meso-pores with nanosize. Therefore, the dehydration process of β -Co(OH)₂ leads to the formation of porosity structure and controllable calcination process realized the preserving of hierarchical nanostructures.

In order to future research the phase transformation of these petals, Three HRTEM images and selected area diffraction pattern (SAED) patterns of β -Co(OH)₂ precursor and Co₃O₄ samples annealing at 280 and 520 °C from red areas in Fig. 4(a, b, f) were analyzed comparatively in Fig. 5. Precursor showed a highly crystalline character with a considerably distinct lattice spacing of 0.275 nm which corresponds to the value of the (100) plane of β -Co(OH)₂ and perfect SAED pattern inset in Fig. 5(a). Co₃O₄ products annealing at 280 °C was found (111) plane corresponding to the *d* value of 0.469 nm and (220) corresponding to 0.286 nm in Fig. 5(b). Judging from its various crystal planes in HRTEM image and inset SAED pattern, it can be figured out that this calcining temperature tended to cause polycrystal Co₃O₄ structure. Fig. 5(c) indicated that Co₃O₄ products for 520 °C perfectly crystallized with *d* value of 0.285 nm corresponding to (220) and inset single crystal SAED pattern. Through the

contrastive analysis of two crystal structural models $\beta\text{-Co(OH)}_2$ and Co_3O_4 in Fig. 5(d), the whole structure transformation process caused the close-packed plane of atoms (001) in brucite-like $\beta\text{-Co(OH)}_2$ transforming into the close-packed plane (111) in spinel-structured Co_3O_4 , which indicated that the [111] axes of spinel nanocrystals are parallel to the [0001] axis of hexagonal $\beta\text{-Co(OH)}_2$. Combined the structure changes from Fig. 5(a-c), it can help to demonstrate spinel-structured Co_3O_4 have a possible topotactic nucleation and crystallization with their [111] directions inheriting the [0001] direction of hexagonal structured $\beta\text{-Co(OH)}_2$.^{9,17}

On the comprehensive observation of morphologies and phases transformation from $\beta\text{-Co(OH)}_2$ to Co_3O_4 , it is suggested that the formation of Co_3O_4 rose-like flower with porous texture is attributed to an in-situ $\beta\text{-Co(OH)}_2$ -to- Co_3O_4 topotactic conversion because of [0001] $\beta\text{-Co(OH)}_2$ /[111] Co_3O_4 (Fig. 5(d)). The single-crystal $\beta\text{-Co(OH)}_2$ petals that assembling into china-rose-like flowers were employed as an in-situ solid-state precursor and template throughout the transformation process.

Thermal decomposition of pure AP shows three stages according to DTA&DSC&TG data in previous literature. The endothermic peak (ENP) appears in the first stage at about 240 °C, ascribed to its transition from orthorhombic form to cubic form. The weak exothermic peak (WEXP) corresponding to the second stage at about 373 °C is attributed to the partial decomposition of AP and the formation of an intermediate product. The further and complete decomposition of the intermediate products was indicated at relatively higher temperature of about 430 °C at the main exothermic peak (MEXP).^{14, 22, 23} And our previous research concerning with the thermal

decomposition of AP was consistent with the above referred work.²⁴

The DSC curves in Fig. 5(a) for thermal decomposition of AP (TDAP) in the presence of Co_3O_4 products annealed at different temperatures, showed noticeable differences in the decomposition patterns of AP. These Co_3O_4 additives all occupied 4% w/w of AP. The ENP appearing in all samples exhibited a similar shape near 240 °C. Therefore, the presence of Co_3O_4 products annealed at different temperature had little influence on the crystallographic phase transition temperature of AP. However, as found in the DSC curves, all the Co_3O_4 catalysts markedly decreased the temperature of TDAP process. Surprisingly, the temperature of MEXP (245~278 °C) with Co_3O_4 additives corresponding to complete decomposition was even much lower than that of WEXP (373.4 °C) in pure AP to partial dissociation. Under similar experimental condition, catalyzed thermal sensitization of AP for this magnitude has only been reported by R. Arun. Chandru group who took mesoporous $\beta\text{-MnO}_2$ powders as catalyst lowering the MEXP temperature to 265 °C.¹⁵ However, Co_3O_4 product annealing at 280 °C in this research lowered the MEXP temperature of AP to 245 °C, which showed the best in catalyzed thermal sensitization of AP by far. Furthermore, with the increase of annealing temperature for Co_3O_4 products, the corresponding catalytic properties worsen gradually. When the annealing temperature was reached up to 520 °C, Co_3O_4 product still could lower the MEXP temperature of AP to 278 °C. Such enhanced lowering of the TDAP regime in the presence of Co_3O_4 additives annealed at different temperatures was also corroborated using Thermo-Gravimetry (TG) (Fig. 5(b)).

BET surface area of the prepared mesoporous Co_3O_4 catalysts annealing at different temperatures were tested. They are 62.9, 36.2, 27.9, 18.3 and 12.65 m^2/g , corresponding to heat treatment temperature of 280, 360, 400, 440 and 520 $^\circ\text{C}$ respectively. The variation trends of BET and decomposition temperature along with annealing temperature were showed in Fig. 5(c). It can be clearly found that BET surface area decreased and the decomposition temperature for AP increased with the increase of annealing temperature. Therefore, the relationship between process and properties could be deduced: higher annealing temperature would lead to the decrease of BET surface area of Co_3O_4 catalysts, and then bring about the worse catalytic performance.

Admirable catalytic performance of flower-like particle was fortunately found, the regular change trend of catalytic performance along with annealing temperature was aroused great interest at the same time. By observing the morphology, the texture of the assembled unit and the change of crystal structure under different annealing temperature, the relationship between the properties and these factors was analyzed and concluded. Keeping the flower-like framework even under different annealing temperature is the premise to its good performance. It was the high specific surface area of this kind of flower-like structure that made the thermal decomposition temperature of AP decreased by at least 140 $^\circ\text{C}$. However, the dehydration process of $\beta\text{-Co}(\text{OH})_2$ and its topotactic conversion into Co_3O_4 also influenced its catalytic performance. When the annealing temperature was 280 $^\circ\text{C}$, relevant Co_3O_4 product was in the initial stage of nucleation and crystallization, with polycrystal structure and

mass crystal defects that help more sites to be active in catalytic process, then it showed the best performance. When the calcining temperature was higher, crystallization was more sufficient, its specific surface area and crystal defects reduced, then exhibiting relatively weaker performance.

4. Conclusions

In conclusion, China rose-like structured β -Co(OH)₂ was successfully prepared by the solvothermal process without surfactant. Its growth process was considered to include three steps: nucleation of hexagonal micro-disks, its growth into platelets and the self-assembly process from platelets into flower-like structure. The structure transformation from brucite-like β -Co(OH)₂ to spinel Co₃O₄ was realized through post annealing treatment without destroying its intrinsic flower-like framework. Specific surface area of Co₃O₄ products decreased as the annealing temperature increased. Meantime, the change of fine texture of petal-like flakelets was found to accompany with cracks propagation and following cavitation. Possible topotactic conversion of β -Co(OH)₂ into Co₃O₄ owing to [0001] β -Co(OH)₂//[111] Co₃O₄ was analyzed. The obtained Co₃O₄ annealing at 280 °C could lower the thermal decomposition temperature of AP to 245 °C, exhibiting the excellent property in catalyzed thermal sensitization of AP. This excellent performance implies great practical significance in the development of solid rocket fuel. Influence of heat treatment on the specific surface area, fine texture and structure transformation of flower-like Co₃O₄ products was also systematically investigated.

Acknowledgements

The authors gratefully acknowledge the financial support from the National Natural Science Foundation of China (Grant No. 51272119) and Beijing Institute of Technology Research Fund Program for Young Scholars.

Notes and references

- 1 H. S. Jadhav, A. K. Rai, J. Y. Lee, J. Kim and C. Park, *Electrochim. Acta*, 2014, 146, 270–277.
- 2 D. Su, S. Dou and G. Wang, *Sci. Rep.*, 2014, 4, 5767, 1-9.
- 3 D. Ghosh, S. Giri, and C. K. Das, *Environ. Prog. Sustain. Energy*, 2014, 33, 1059-1064.
- 4 W. Y. Li, L. N. Xu, J. Chen, *Adv. Funct. Mater.*, 2005, 15, 851-857.
- 5 M. J. Liao, J. Y. Feng, W. J. Luo, Z. Q. Wang, J. Y. Zhang, Z. S. Li, T. Yu and Z. G. Zou, *Adv. Funct. Mater.*, 2012, 22, 3066–3074.
- 6 Q. Y. Yan, X. Y. Li, Q. D. Zhao and G. H. Chen, *J. Hazard. Mater.*, 2012, 210, 385–391.
- 7 M. S. Wang, L. K. Zeng and Q. W. Chen, *Dalton Trans.*, 2011, 40, 597–601.
- 8 J. S. Chen, T. Zhu, Q. H. Hu, J. Gao, F. Su, S. Z. Qiao, and X. W. Lou, *ACS Appl. Mater. Interfaces*, 2010, 12, 3628–3635.
- 9 L. Tian, H. L. Zou, J. X. Fu, X. F. Yang, Y. Wang, H. L. Guo, X. H. Fu, C. L. Liang, M. M. Wu, P. K. Shen, and Q. M. Gao, *Adv. Funct. Mater.*, 2010, 20, 617-623.
- 10 Y. Liu, C. Mi, L. Su and X. Zhang, *Electrochim. Acta*, 2008, 53, 2507-2513.
- 11 Y. Li, B. Tan and Y. Wu, *NanoLett.*, 2008, 8, 265-270.
- 12 K. T. Nam, D. W. Kim, P. J. Yoo, C. Y. Chiang, N. Meethong, P. T. Hammond, Y.

- M. Chiang and A. M. Belcher, *Science*, 2006, 312, 885-888.
- 13 T. A. Mulinari, F. A. L. Porta, J. Andre's, M. Cilense, J. A. Varela and E. Longo, *CrystEngComm.*, 2013, 15, 7443-7449.
- 14 N. Li, Z. F. Geng, M. H. Cao, L. Ren, X. Y. Zhao, B. Liu, Y. Tian and C. W. Hu, *Carbon*, 2013, 54,124 –132.
- 15 R. A. Chandru, S. Patra, C. O. Municandrai and B. N. Raghunandan, *J. Mater. Chem.*, 2012, 22, 6536–6538.
- 16 Y. Yuan, W. Jiang, Y. J. Wang, P. Shen, F. S. Li, P. Y. Li, F. Q. Zhao and H. X. Gao, *Appl. Surf. Sci.*, 2014, 303, 354–359.
- 17 L. Tian, X. Yang, P. Lu, I. D. Williams, C. Wang, S. Ou, C. Liang, and M. Wu, *Inorg. Chem.*, 2008, 47, 5522-5524.
- 18 Y. F. Zhang, M. Z. Ma, X. Y. Zhang, B. Wang and R. P. Liu, *J. Alloy Compd.*, 2014, 590, 373–379.
- 19 X. Y. Jing, S. S. Song, J. Wang, L. Ge, S. Jamil, Q. Liu, T. Mann, Y. He, M. L. Zhang, H. Wei and L. H. Liu, *Powder Technol.*, 2012, 217, 624–628.
- 20 C. Mondal, M. Ganguly, P. K. Manna, S. M. Yusuf and T. Pal, *Langmuir*, 2013, 29, 9179–9187.
- 21 G. S. Cao, X. J. Zhang and L. Su, *Bull. Mater.Sci.*, 2011, 34, 973–977.
- 22 R. DL, R. AE, C. RV, S. MA, L. AR and S. TC, *NanoLett.*, 2007, 7, 2157-2561.
- 23 L. M. Song, S. J. Zhang, B. Chen, J. J. Ge and X. C. Jia, *Colloids Surf., A*, 2010, 360, 1-5.
- 24 X. Xu, Y. Zhao, J. Li, H. B. Jin, Y. Zhao and H. Zhou, *Mater. Res Bull.*, 2015, 72,

7–12.

Figure Captions:

Fig.1 (a-c) SEM images of β -Co(OH)₂ China rose-like flowers with different magnifications; (d) XRD patterns of as-prepared product samples; (e) TEM image of the nanosheet in the β -Co(OH)₂ flower; (f) HRTEM image of the red-marked area and corresponding selected area electron diffraction (SAED) pattern.

Fig.2 SEM images of the time-dependent evolution in the form of β -Co(OH)₂ China rose-like flowers. (a) 2 h; (b) 12 h; (c) 24 h; (d) Schematic illustration of the β -Co(OH)₂ with flower-like structures formation process. Steps: (1) the formation and growth of β -Co(OH)₂ microdisks; (2) the shape evolution of β -Co(OH)₂ microdisks; (3) The nano petal self-assembly process into β -Co(OH)₂ China rose-like flowers.

Fig.3 Powder XRD patterns of precursor β -Co(OH)₂ nanobelts and products by annealing the precursor in air at temperatures of 280, 360, 400, 440 and 550 °C, respectively.

Fig.4 Low magnification TEM images and low magnification SEM images of β -Co(OH)₂ precursor and Co₃O₄ samples annealing at different temperatures: (a) precursor; (b) 280 °C; (c) 360 °C; (d) 400 °C; (e) 440 °C; (f) 520 °C; (g) Fine texture transformation schematic of petal.

Fig.5 High magnification TEM images and corresponding selected area diffraction pattern (SAED) patterns of β -Co(OH)₂ precursor and Co₃O₄ samples annealing at different temperatures (All selected areas found in Fig. 4(a, b, f) respectively): (a) precursor; (b) 280 °C; (c) 520 °C; (d) crystal structure transformation mechanism of nano petal.

Fig.6 (a) The DSC curves for mixtures of AP and Co₃O₄ calcined at different temperatures: (a1) 280 °C; (a2) 360 °C; (a3) 400 °C; (a4) 440 °C; (a5) 520 °C; (b)

Corresponding TG curves for mixtures of AP and Co_3O_4 ; (c) The BET and Decomposition Temperature change curves along with Annealing Temperature.

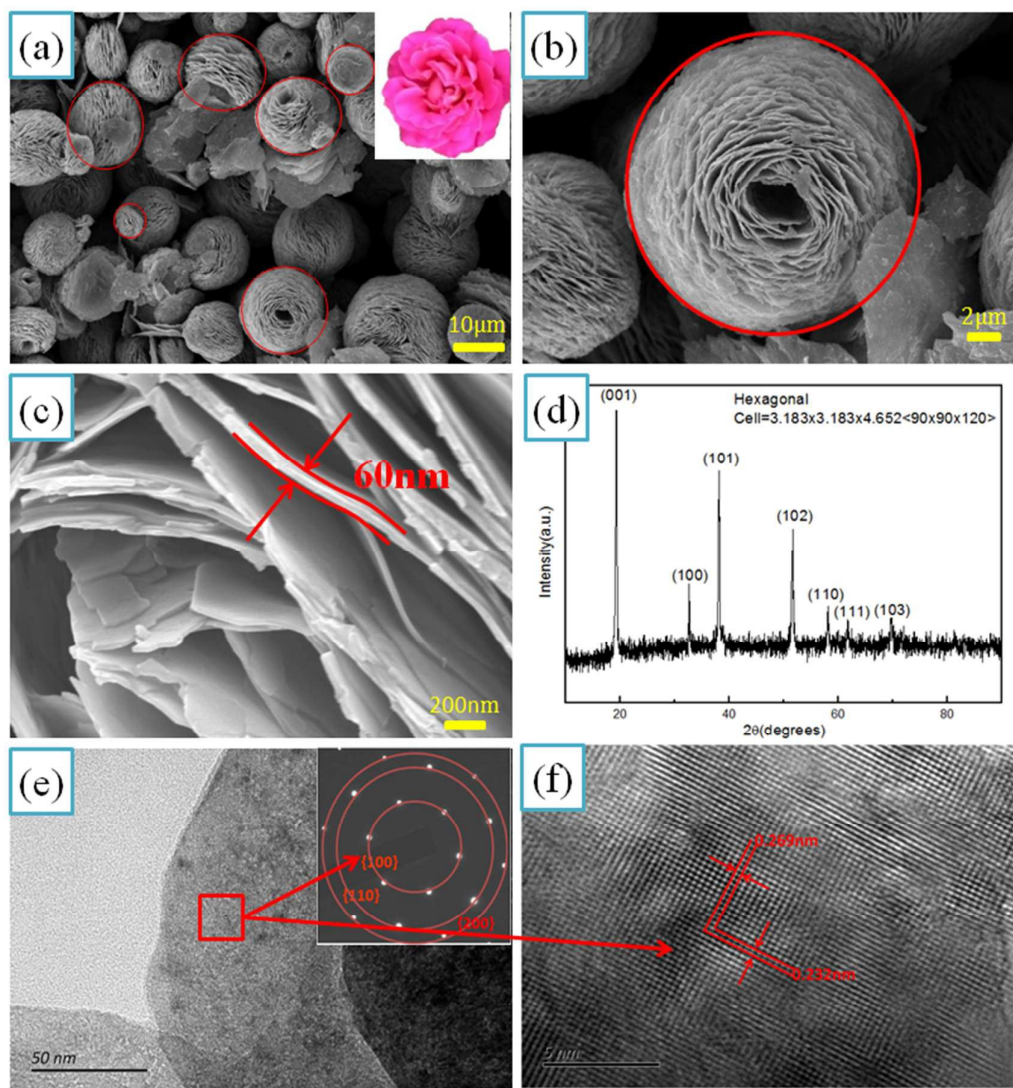


Fig.1 (a-c) SEM images of β -Co(OH)₂ China rose-like flowers with different magnifications; (d) XRD pattern of as-prepared product sample; (e) TEM image of the nanosheet in the β -Co(OH)₂ flower; (f) HRTEM image of the red-marked area and corresponding selected area electron diffraction (SAED) pattern.

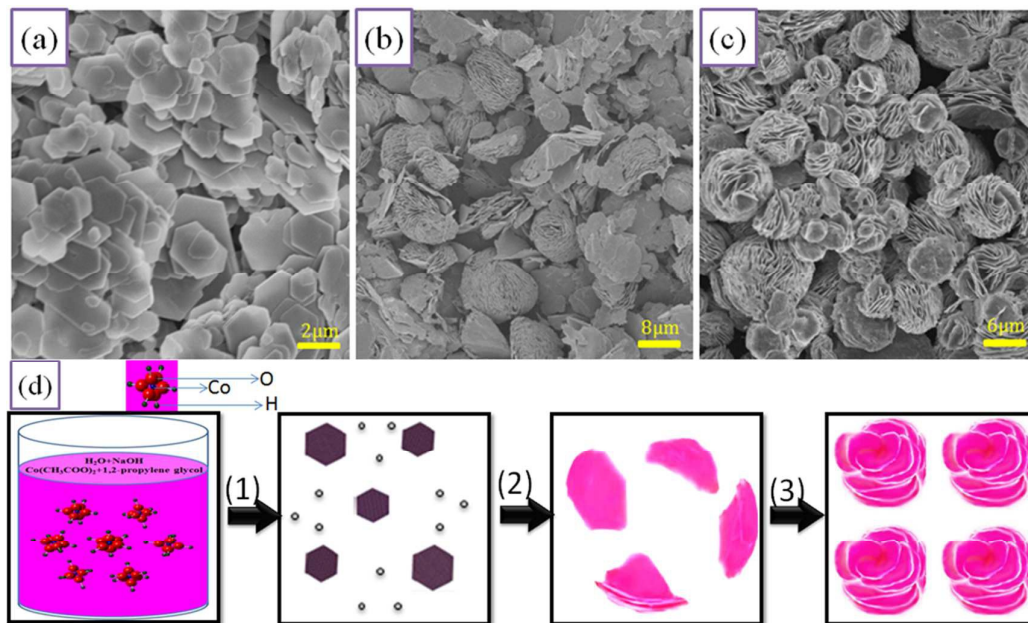


Fig.2 SEM images of the time-dependent evolution in the form of β -Co(OH)₂ China rose-like flowers. (a) 2 h; (b) 12 h; (c) 24 h; (d) Schematic illustration of the β -Co(OH)₂ with flower-like structures formation process. Steps: (1) the formation and growth of β -Co(OH)₂ microdisks; (2) the shape evolution of β -Co(OH)₂ microdisks; (3) The nano petal self-assembly process into β -Co(OH)₂ China rose-like flowers.

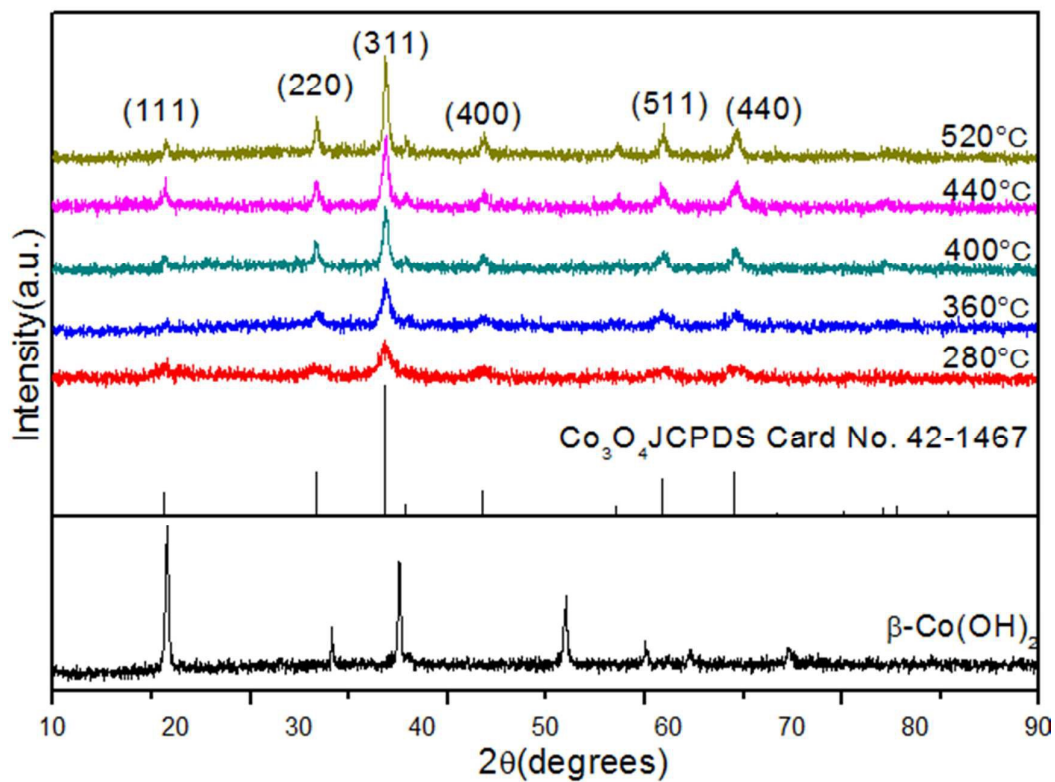


Fig.3 Powder XRD patterns of precursor $\beta\text{-Co(OH)}_2$ and products by calcining the precursor in air at temperatures of 280, 360, 400, 440 and 550 °C, respectively.

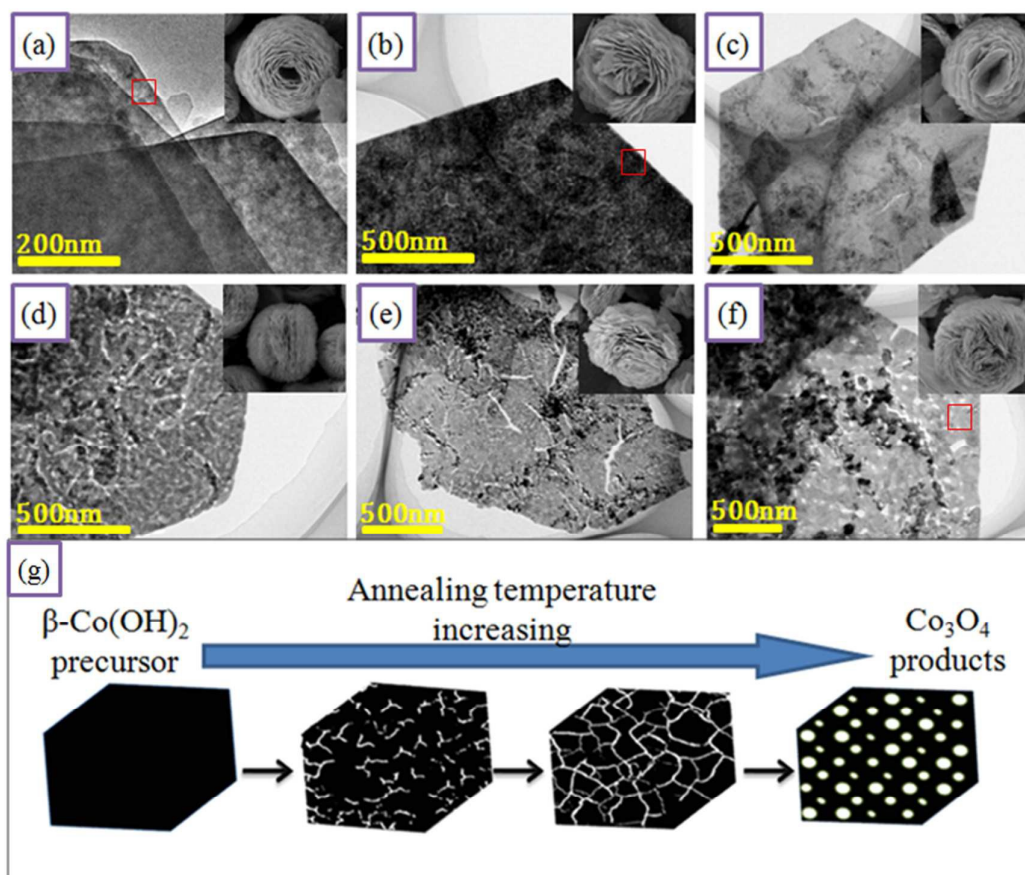


Fig.4 Low magnification TEM images and low magnification SEM images of β -Co(OH)₂ precursor and Co₃O₄ samples annealing at different temperatures: (a) precursor; (b) 280 °C; (c) 360 °C; (d) 400 °C; (e) 440 °C; (f) 520 °C; (g) Fine texture transformation schematic of petal.

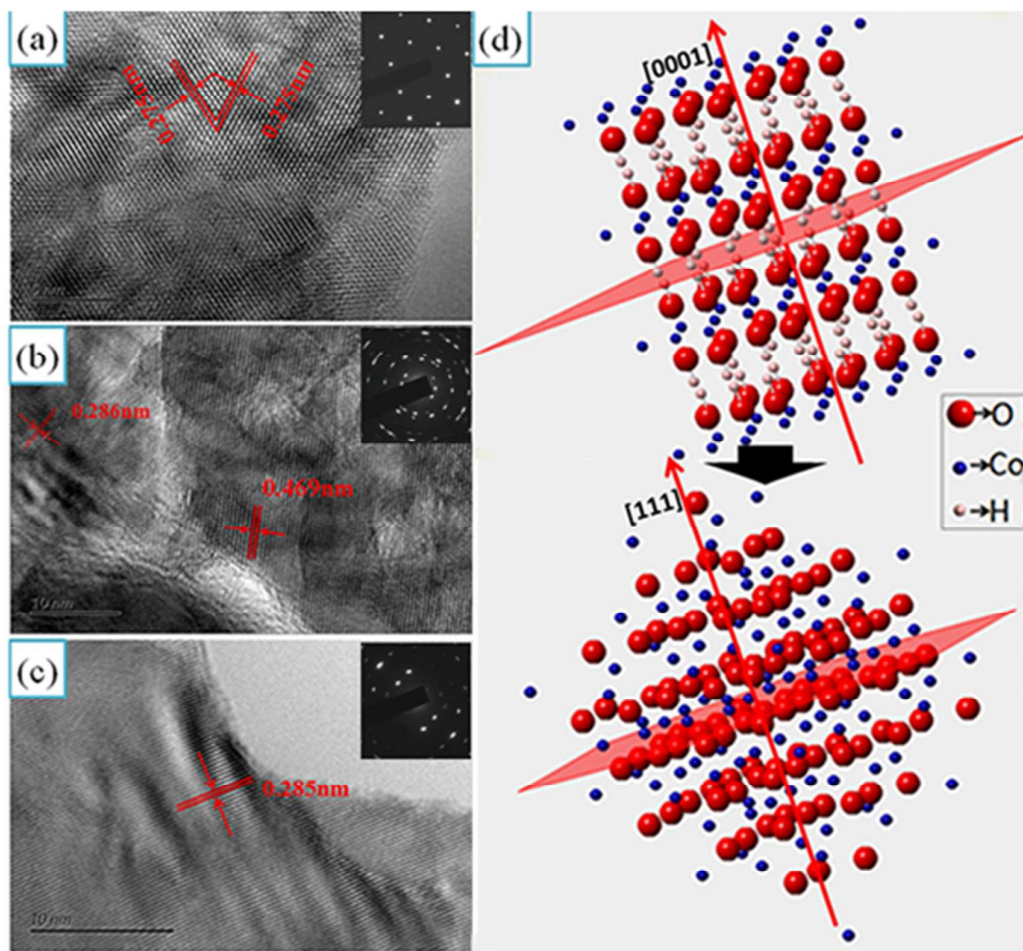


Fig.5 High magnification TEM images and corresponding selected area diffraction pattern (SAED) patterns of β -Co(OH)₂ precursor and Co₃O₄ samples annealing at different temperatures (All selected areas found in Fig. 4(a, b, f) respectively): (a) precursor; (b) 280 °C; (c) 520 °C; (d) crystal structure transformation mechanism of nano petal.

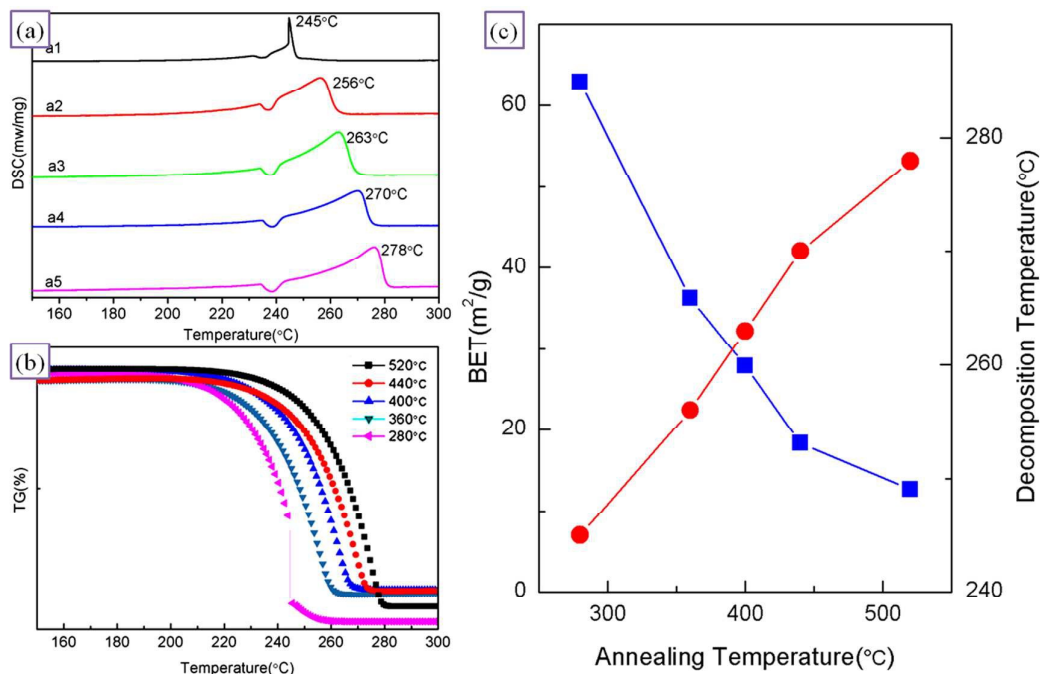


Fig.6 (a) The DSC curves for mixtures of AP and Co_3O_4 calcined at different temperatures: (a1) 280°C; (a2) 360 °C; (a3) 400 °C; (a4) 440 °C; (a5) 520 °C; (b) Corresponding TG curves for mixtures of AP and Co_3O_4 ; (c) The BET and Decomposition Temperature change curves along with Annealing Temperature.

Graphical Abstract

